Journal of
Ceramic Science
and Technology

J. Ceram. Sci. Technol., **12** [2] 97-106 (2021)
DOI: 10.4416/JCST2020-00028
available online at: http://www.ceramic-science.com

The Effect of Sintering Temperature on the Phase Composition and Mechanical Properties of Al_2O_3-TiC-TiN Ceramic Tool Materials

Yuhuan Fei*[1, 2], Chuanzhen Huang[3, 4], Hanlian Liu[4], Tianen YANG[5], Jikang XU[6]

[1]School of Engineering, Qufu Normal University, Rizhao 276826, P. R. China
[2]Rizhao Huilian Zhongchuang Institute of Intelligent Technology, Rizhao 276826, P. R. China
[3]School of Mechanical Engineering, Yanshan University, Qinhuangdao 066004, P. R. China
[4]Center for Advanced Jet Engineering Technologies (CaJET), Key Laboratory of High-efficiency and Clean Mechanical Manufacture (Ministry of Education), National Experimental Teaching Demonstration Center for Mechanical Engineering (Shandong University), School of Mechanical Engineering, Shandong University, Jinan 250061, P. R. China
[5]School of Mechanical Engineering, Sichuan University, Chengdu 610065, P. R. China
[6]College of Transportion, Shandong University of Science and Technology, Qingdao 266590, P.R. China
received December 22, 2020; received in revised form May 15, 2021; accepted May 27, 2021

Abstract

Al_2O_3-20 vol% TiC-10 vol% TiN ceramic tool materials were fabricated with the hot-pressing technique at different sintering temperatures. The effects of the sintering temperature on the phase composition, mechanical properties, and microstructure were investigated. The results have shown that hexagonal-Mo_3C_2 and tetragonal-$AlNi_3$ adversely affected the mechanical properties overall. Orthorhombic-MoNi and cubic-$AlNi_3$ were able to improve the flexural strength and hardness, but cubic-$AlNi_3$ decreased the fracture toughness. When the ceramic materials were sintered with the holding time of 10 minutes and sintering pressure of 32 MPa, all mechanical properties changed in the same way with the increment of the sintering temperature. The highest flexural strength of 807.4 MPa was measured when the sintering temperature was 1 650 °C, the highest Vickers hardness of 20.78 GPa was measured when the sintering temperature was 1 700 °C, the highest fracture toughness of 7.58 MPa·m$^{1/2}$ was measured when the sintering temperature was 1 500 °C. The overall mechanical properties were optimal when the sintering temperature was 1 500 °C, at which the mechanical properties were 796.6 MPa, 20.5 GPa, 7.58 MPa·m$^{1/2}$ for flexural strength, Vickers hardness, and fracture toughness, respectively.

Keywords: Al_2O_3-TiC-TiN, sintering temperature, phase composition, mechanical properties

I. Introduction

High-speed machining is used more and more widely since it can enhance productivity, improve quality, increase the material removal rate, and lower cost significantly. The cutting speed for high-speed machining of steel can reach 300 ~ 800 m/min [1, 2]. When machining steel with high speed, ceramic cutting tool materials demonstrate excellent performance, such as high red-hardness, wear resistance, and oxidation resistance [3, 4, 5]. Al_2O_3-matrix ceramics are especially suited for cutting quenched steel at high speed [6, 7, 8, 9].

The inherent brittleness of alumina ceramics has limited their applications, but Al_2O_3-matrix composites with different additives exhibit better mechanical properties. The additives for Al_2O_3-matrix ceramics include reinforced phase, toughening phase, sintering aids, metal binders and so on. TiC [9, 10, 11] and TiN [11, 12, 13, 14] are commonly used as secondary phases, since they can improve flexural strength and hardness. MgO [15, 16, 17, 18] and Y_2O_3 [18, 19, 20] are most commonly used as sintering aids because they can decrease the sintering temperature and inhibit grain growth. Ni, Co, and Mo are mostly used as binders to accelerate the sintering process and increase toughness [21, 22, 23, 24, 25].

The Al_2O_3-TiC-TiN material system had been studied in previous work [17, 21, 26, 27]. The ceramic cutting tool materials were fabricated with the hot-pressing technique and with varying content of the different components. The results showed that with the sintering temperature of 1 600 °C, holding time of 10 minutes, and the pressure of 32 MPa, the overall mechanical properties and cutting performance were good when the volume content of TiC was 20 vol%, the volume content of TiN was 10 vol%, the volume content of MgO was 1 vol%, the volume content of Mo was 1 vol%, and the volume content of Ni was 1 vol%, respectively.

Besides the material composition, the sintering parameters are also important factors influencing the material's mechanical properties. In the present work, different sintering temperatures were applied for the material system described above. The composites thus obtained were characterized based on their microstructure, phase com-

* Corresponding author: yuhuanfei@qfnu.edu.cn

position, and mechanical properties. The microstructure of the ceramics was observed by means of scanning electron microscopy (SEM), the phase composition of the sintering body was analysed with X-ray diffraction (XRD), the mechanical properties, such as flexural strength, Vickers hardness, and fracture toughness, were evaluated. Particular emphasis was placed on studying the effects of the sintering parameters on the phase composition, mechanical properties and microstructure of Al_2O_3-20 vol% TiC-10 vol% TiN ceramic materials.

II. Experiments

(1) Starting materials and sample preparation

The specifications of the raw materials are listed in Table 1. The combination of the raw materials was mixed using ethyl alcohol as a solvent, and the compounds were homogenized for 48 hours in a ball mill with alumina balls. Then the slurries were dried in a vacuum oven (Moder ZK-82A), and a 100-mesh sieve was used to obtain the powders. In order to produce ceramic disks, the compacted powders were ultimately densified by hot pressing in the ZRC85 – 25T sintering furnace. With reference to experience, the sintering temperature we applied for hot pressing ranged from 1 500 °C to 1 750 °C, at 50 K intervals. The holding time was 10 minutes and the sintering pressure was 32 MPa.

Each sintering experiment was repeated at least three times to provide enough ceramic disks for the following work.

(2) Characterization techniques

The ceramic disks were cut into bars with a diamond slicing machine (J5060CE1), then the bars were ground into rectangular bar specimens (4 mm × 3 mm × 30 mm). A universal testing machine (WDW-50E) was used to perform three-point bending tests and measure the flexural strength at room temperature. The test span was 20 mm and the crosshead speed was 0.5 mm/min. Measurements of the Vickers hardness and the fracture toughness were calculated based on the direct indentation method. The indentation on the polished surface of the samples was obtained with a Vickers hardness testing machine (HVS-50) using a pyramid indenter. The indentation load applied was 196 N and the holding time was 15 s. For each specimen, the three-point bending test was performed at least six times, while the indentation test was performed at least ten times.

A scanning electron microscope with energy-dispersive spectrometry (ZEISS SUPRA-55) was used to observe the microstructures of the ceramics, which included polished and fracture surfaces. XRD analysis was conducted using a diffractometer (D/max-rb) with copper K_α radiation. The phase composition of the sintered ceramic materials was determined based on comparison with the standard values from the International Centre for Diffraction Data's Powder Diffraction File (JCPDS).

III. Results and Discussion

(1) Phase composition

Fig. 1 shows the X-ray diffraction results of the six ceramic materials fabricated at different temperatures, and Table 2 lists the details of the phase components in each material.

It indicates that all ceramic materials had Al_2O_3 phase maintaining the original lattice structure, but other components had different products and a variety of lattice structures.

When the sintering temperature was 1 500 °C, TiC and TiN dissolved completely and generated $TiC_{0.51}N_{0.12}$ (hexagonal system). Mo changed to MoNi (orthorhombic system) with part of the Ni atoms. The remaining Ni atoms changed to $AlNi_3$ (cubic system). The lattice structure of $AlNi_3$ is the same as that of Ni, but the lattice volume is larger than that of Ni. Mg element finally existed in the form of $Mg_{0.388}Al_{2.408}O_4$ (cubic system). Mo is a strong soluble element of Ni, when Mo atoms enter the lattice of Ni, they can slow the softening speed. As a consequence, the heat-resisting strength of the material can be improved. Shi *et al.* [28] calculated the heats of formation of six Ni-Al intermetallic compounds, and the values indicated a very strong chemical interaction between Al and Ni. $AlNi_3$ is an ordered intermetallic with the $L1_2$ lattice structure. Aluminium is the dominant diffusing element during Al_3Ni growth, Al atoms can cause lattice distortion of Ni. As a result, the strength of the material can be increased. Meanwhile, non-deformable particles have the Orowan mechanism, and the deformable particles have the dislocation mechanism, so the intermetallic compounds of Al and Ni can cause a precipitation hardening effect [29, 30]. $Mg_{0.388}Al_{2.408}O_4$ is Al_2O_3-rich spinel is formed as a result of the cation defect ($3Mg^{2+}$and $2Al^{3+}$), and the lattice volume of $Mg_{0.388}Al_{2.408}$ is larger than that of the MgO.

Table 1: Specifications of the raw materials

Components	Volume content	Purity	Mean particle size (μm)	Density (g/cm^3)	Manufacture
Al_2O_3	0.67	99.9%	0.50	3.99	Zibo, China
TiC	0.20	>99.0%	0.50	4.93	Hefei, China
TiN	0.10	>99.0%	0.50	5.43	Hefei, China
MgO	0.01	≥98.0%	1.52	3.58	Tianjin, China
Ni	0.01	≥99.5%	2.30	8.90	Beijing, China
Mo	0.01	≥99.7%	2.30	10.20	Beijing, China

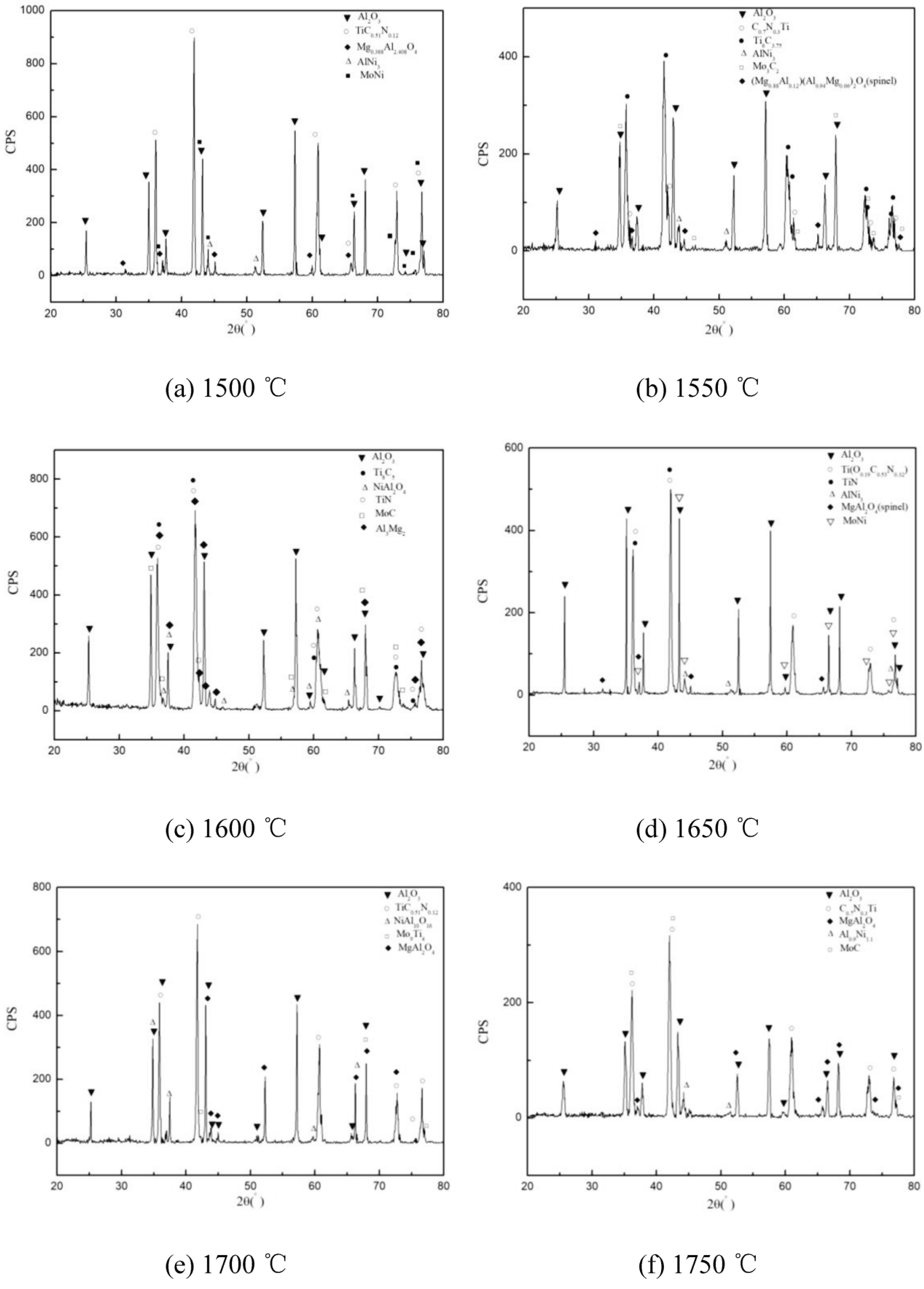

Fig. 1: The X-ray diffraction results for the sintered materials (10 min, 32 MPa).

Table 2: The phase composition of the sintered ceramic materials

Sintering temperature	Al_2O_3	TiC	TiN	Mo	Ni	MgO
1 500 °C	Al_2O_3	$TiC_{0.51}N_{0.12}$		MoNi	cubic-$AlNi_3$	$Mg_{0.388}Al_{2.408}O_4$
1 550 °C	Al_2O_3	$Ti_6C_{3.75}$	$C_{0.7}N_{0.3}Ti$	Mo_3C_2	tetragonal-$AlNi_3$	$(Mg_{0.88}Al_{0.12})(Al_{0.94}Mg_{0.06})_2O_4$
1 600 °C	Al_2O_3	Ti_8C_5	TiN	hexagonal-MoC	$NiAl_2O_4$	Al_3Mg_2
1 650 °C	Al_2O_3	$Ti(O_{0.19}C_{0.53}N_{0.32})$	TiN	MoNi	cubic-$AlNi_3$	spinel-$MgAl_2O_4$
1 700 °C	Al_2O_3	$TiC_{0.51}N_{0.12}$		Mo_9Ti_4	$NiAl_{10}O_{16}$	$MgAl_2O_4$
1 750 °C	Al_2O_3	$C_{0.7}N_{0.3}Ti$		Cubic-MoC	cubic-$AlNi_3$	$MgAl_2O_4$

When the sintering temperature was increased to 1 550 °C, the original TiN became $C_{0.7}N_{0.3}Ti$ solution (cubic system) with part of the TiC, while the remaining TiC changed to $Ti_6C_{3.75}$ (hexagonal system). Mg element finally existed in the form of $(Mg_{0.88}Al_{0.12})(Al_{0.94}Mg_{0.06})_2O_4$ (cubic system), which is a kind of incomplete spinel. Decarbonization of TiC occurred during the sintering process, then Mo element combined with the C element and generated Mo_3C_2 (hexagonal system). Ni element existed in the form of $AlNi_3$ (tetragonal system). Each crystal system has a specific lattice structure, so tetragonal-$AlNi_3$ and cubic-$AlNi_3$ may affect the mechanical properties in different ways. The lattice volume of tetragonal-$AlNi_3$ is larger than that of cubic-$AlNi_3$. Both tetragonal-$AlNi_3$ and hexagonal-Mo_3C_2 are interstitial phases, they cause brittleness and impair the mechanical properties.

When the sintering temperature was increased to 1 600 °C, Ti_8C_5 (rhombohedral system)was generated, and TiN retained the original lattice structure. After sintering, Mg element existed in the form of Al_3Mg_2 (cubic system). There was also decarbonization of TiC and the C element combined with the Mo element. However, the two elements generated MoC (hexagonal system), not Mo_3C_2 (hexagonal system), which was generated at 1 550 °C. The intermetallic compound Al_3Mg_2 has a complex face-centred cubic structure, with a giant unit cell containing about 1 168 atoms [31]. Al_3Mg_2 is usually considered as a brittle phase, which can adversely affect strength and toughness. However, Straumal's research showed that Al_3Mg_2 could wet the Al/Al grain boundaries, thus enhancing the hardness of the materials [32].

When the sintering temperature was increased to 1 650 °C, the original TiC became $Ti(O_{0.19}C_{0.53}N_{0.32})$ (cubic system), the remaining TiN kept the same phase as the raw materials. Mg element finally existed in the form of spinel-$MgAl_2O_4$ (cubic system). Ni element existed in the forms of orthorhombic-MoNi and cubic-$AlNi_3$, which were the same as the products sintered at 1 500 °C. The research of Lu *et al.* indicated when MgO combined with Al_2O_3 and generated spinel-$MgAl_2O_4$, the microstructure was fine-grained and the bending strength was excellent [18]. The interface energy between the Al_2O_3 and spinel is low, so the diffusion velocity is decreased and the grain growth is restrained. Consequently, spinel-$MgAl_2O_4$ can decrease grain size and improve the sintered density.

When the sintering temperature was increased to 1 700 °C, the original TiN combined with TiC and generated $TiC_{0.51}N_{0.12}$ (hexagonal system), which was the same phase as the product generated at 1 500 °C. Mg element finally existed in the form of $MgAl_2O_4$ (orthorhombic system), which was different from spinel-$MgAl_2O_4$ generated at 1 650 °C. Mo element existed in the form of Mo_9Ti_4 (tetragonal system). The Ni element changed to $NiAl_{10}O_{16}$ (monoclinic system), which is more stable than $NiAl_2O_4$. Mo is the stable element of β-Ti, the lattice of Mo is the same as β-Ti, and the lattice parameters are close. Therefore, when the Mo atoms replace Ti atoms to form Mo_9Ti_4, the lattice distortion is small, so the ductility and toughness are good.

When the sintering temperature increased to 1 750 °C the original TiN combined with TiC and generated $C_{0.7}N_{0.3}Ti$ solution (cubic system), which was the same phase as the product generated at 1 550 °C. Mg element also existed in the form of $MgAl_2O_4$ (orthorhombic system). Decarbonization of TiC occurred during the sintering process again, and the C element combined with Mo element to generate MoC (cubic system), which was different from the MoC (hexagonal system) generated after sintering at 1 600 °C. Ni element existed in the form of $AlNi_3$ (cubic system), which was the same phase as the product at 1 500 °C.

Based on a comparison of the six X-ray diffraction results, we firstly found that when the sintering temperature was higher than 1 600 °C, the TiC phase dissolved completely. When the sintering temperature was higher than 1 650 °C, the TiN phase dissolved completely. According to the research by Paseuth *et al.* [33], the indentation hardness of $C_{0.7}N_{0.3}Ti$ can reach 28.5 GPa, so the existence of $C_{0.7}N_{0.3}Ti$ can improve the hardness of the material. But during the generation of $TiC_{0.51}N_{0.12}$, the Ti atoms easily combine with the liquid phase and form brittle phase, which decreases the strength of the materials.

Secondly, after the sintering process, Ni existed in five forms: MoNi, $AlNi_3$(cubic system), $AlNi_3$ (tetragonal system), spinel- $NiAl_2O_4$, and $NiAl_{10}O_{16}$. Ni atoms tend to combine with multiple elements and form nickel-based solid solution. These solute elements have a strengthening effect based on elastic interaction, chemical interaction, and electron interaction. As a result, the strength and hardness of the materials can be enhanced. As previously mentioned, the compound of Ni and Mo can stabilize the

matrix phase and hard phases. Al atoms can increase the slip resistance because of the distortion of the Ni lattice. Meanwhile the Ni-Al intermetallic compounds can cause a precipitation strengthening effect.

Moreover, with the variation of sintering temperature, the Mo element was also present as multiple phases after the sintering process. The results showed that the Mo element tended to combine with C element, but there were different forms. The details of the phases are listed in Table 3. Hugosson *et al.* [33] predicted the relative stabilities of experimentally verified molybdenum carbides, the result showed that hexagonal-MoC is the most stable phase followed by cubic-MoC and hexagonal Mo_3C_2. However, the mechanism has not yet been understood. Our further work will investigate the phase transition with the help of phase-field-crystal simulation.

Last but not least, the solubility of MgO in the spinel increased with the increment of the sintering temperature. When the sintering temperature was higher than 1 650 °C, MgO combined with Al_2O_3 completely and generated spinel-$MgAl_2O_4$. During the conversion process, there was volume expansion (about 5 % ~ 8 %). Meanwhile, the recrystallization capacity of $MgAl_2O_4$ is weak, which decreases the microstructure compactness, thus adversely affecting the mechanical properties. When the sintering temperature was higher than 1 700 °C, the lattice of $MgAl_2O_4$ stretched along two directions, while it was significantly compressed along another direction, before changing to an orthorhombic system, the lattice volume decreased. Taken as a whole, the lattice of the phases generated by Mg and Mo changed by the same rule, the volume first increased and then decreased with the increment of sintering temperature.

(2) Mechanical properties

In previous work [26], the mechanical properties of Al_2O_3-TiC-TiN ceramic tool materials had been studied. Fig. 2 shows the mechanical properties of the material system in this research. It indicated that all three mechanical properties first decrease, then increase and decrease again with the increment of the sintering temperature. When the sintering temperature was 1 650 °C, the flexural strength was the highest, with a value of 807.4 MPa. When the sintering temperature was 1 700 °C, the Vickers hardness was best, with a value of 20.78 GPa. When the sintering temperature was 1 500 °C, the fracture toughness was highest, with a value of 7.58 MPa·$m^{1/2}$. In general, when the sintering temperature was 1 500 °C, the mechanical properties were the best overall, the flexural strength measuring 796.6 MPa, the Vickers hardness 20.5 GPa, and the fracture toughness 7.58 MPa·$m^{1/2}$.

The relationship between some phases with specific mechanical properties can be inferred from Table 2 and Fig. 2. MoNi (orthorhombic system) can improve the flexural strength and hardness. Mo_3C_2 (hexagonal system) and $AlNi_3$ (tetragonal system) can easily lead to brittleness, thus decreasing the mechanical properties overall. $AlNi_3$ (cubic system) is a typical dispersion-strengthening and binding phase, and it can thus enhance the strength and hardness of the material. However, it will reduce its fracture toughness. Further work is required here to explain this mechanism.

(3) Typical microstructure

The mechanical properties are closely related to the microstructure. Fig. 3 shows typical SEM micrographs of the materials.

Fig. 3(a) shows that when the materials were sintered at 1 500 °C, the microstructure of ceramic material was homogeneous, most of the particles were equiaxial, the mean particle size was about 2 μm. The metal binding phase wetted the big hard-phase particles well, and a special three-layers core-rim structure was observed, which has been marked with a circle. The wetted hard phases were mainly spherical in shape, while the hard phases that had not been wetted were columnar. The columnar particles can be easily pulled out, which can increase the fracture toughness of the material. As shown in Fig. 3(b), we found that the fracture surface had obvious transgranular fracture morphology and many particles were split (marked with a circle).

As shown in Fig. 3(c) and Fig. 3(d), when the sintering temperature was increased to 1 650 °C, the microstructure was non-uniform, some binding phases were distributed close to the hard-phase particles, some short columnar particles existed separately. The hard-phase particles were small and had sharp edges, which could result in a pinning effect, and hence increase the strength of the material. As marked by the arrow, the binding force between the binding phase and hard phase was strong, while they maintained a tight junction even at the fracture surface.

From Fig. 3(e) and Fig. 3(f), it can be seen that when the sintering temperature was 1 700 °C, the compactness of the microstructure was good, hard-phase particles were uniform and dispersed sparsely. There were micro-cracks (marked with a circle) in the big particle, which would increase the fracture toughness.

Table 3. The phase details of the molybdenum carbides

Sintering temperature	Product	Lattice parameters						Pearson symbols	Space group
		a (nm)	b (nm)	c (nm)	α(°)	β(°)	γ(°)		
1 550 °C	Mo_3C_2	0.3016	0.3016	1.464	90	90	120	hP12	$P6_3/mmc$
1 600 °C	hexagonal-MoC	0.2932	0.2932	1.097	90	90	120	hP8	$P6_3/mmc$
1 750 °C	cubic-MoC	0.4273	0.4273	0.4273	90	90	90	cF8	Fm-3m

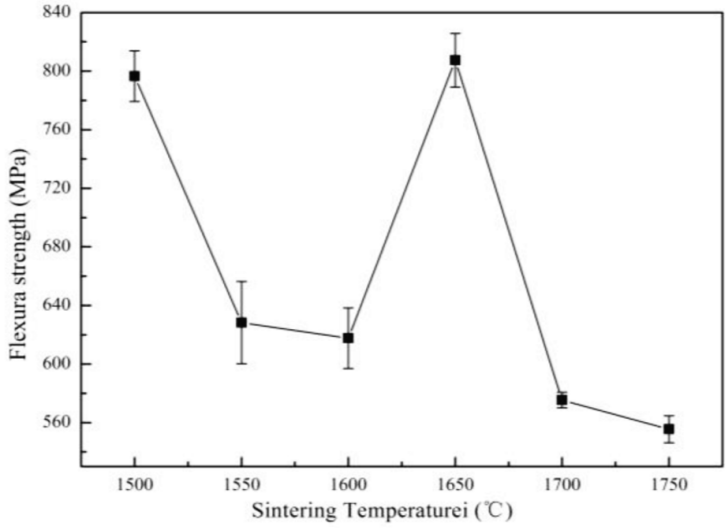

(a) Flexural strength

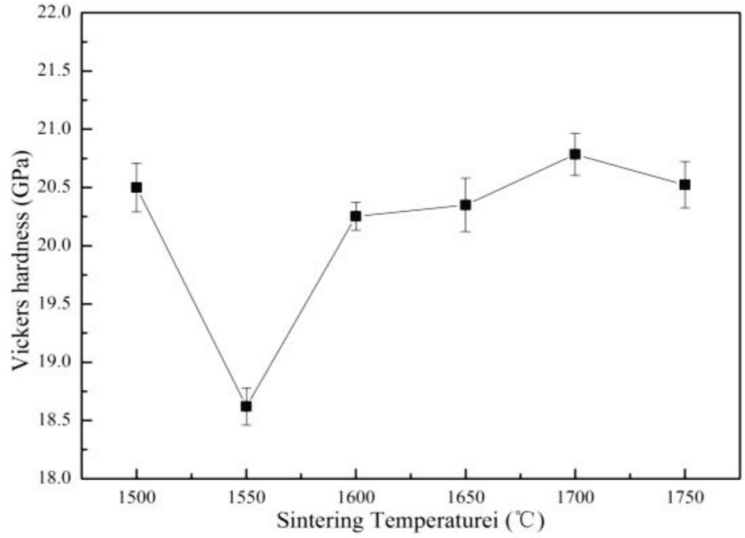

(b) Vickers hardness

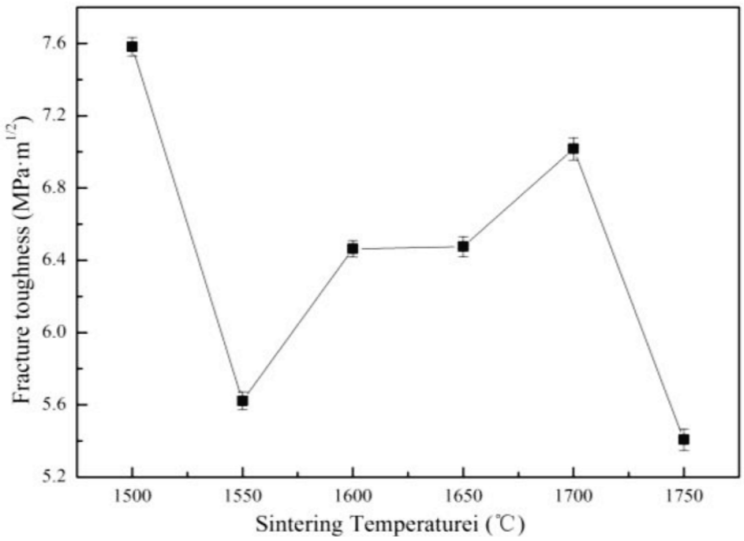

(c) Fracture toughness

Fig. 2: The mechanical properties of the materials (10 min, 32 MPa).

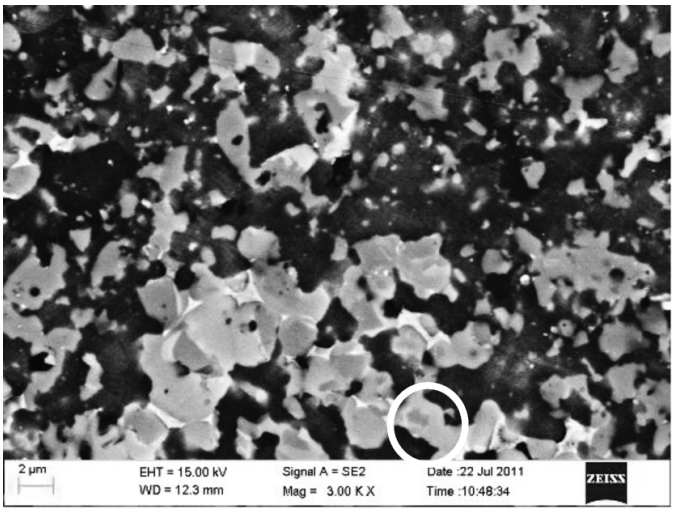

(a) 1500 ℃, polished surface, 3000×

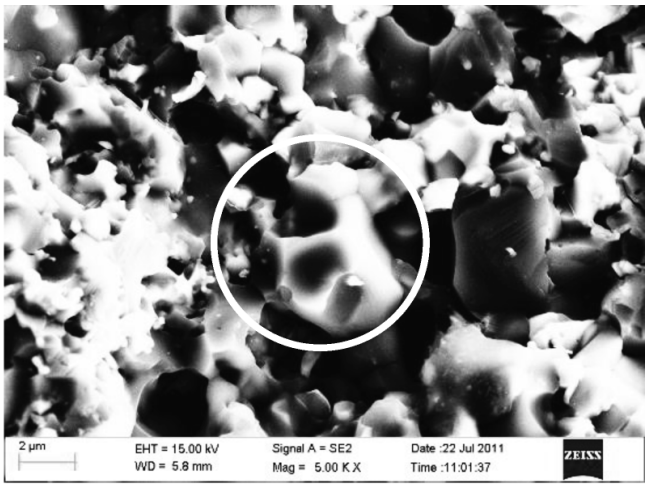

(b) 1500 ℃, fracture surface, 5000×

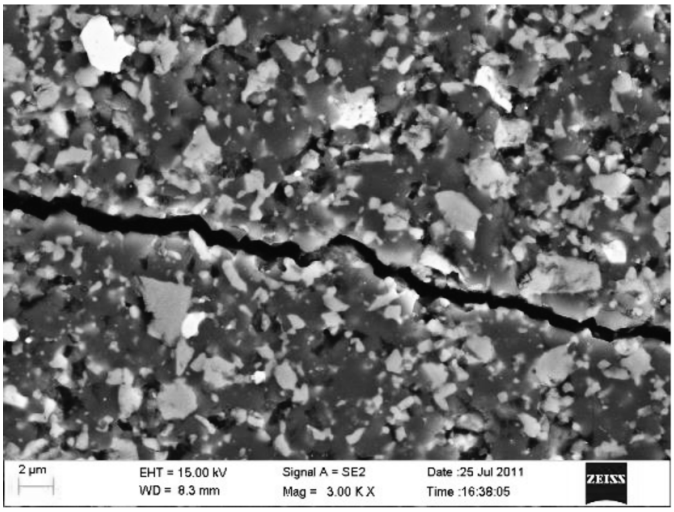

(c) 1650 ℃, polished surface, 3000×

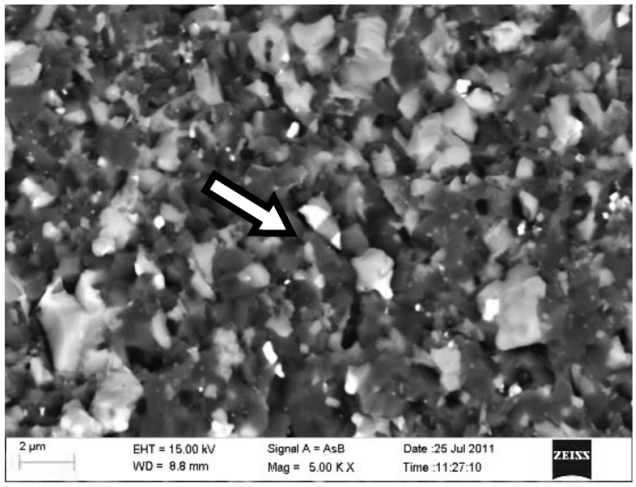

(d) 1650 ℃, fracture surface, 5000×

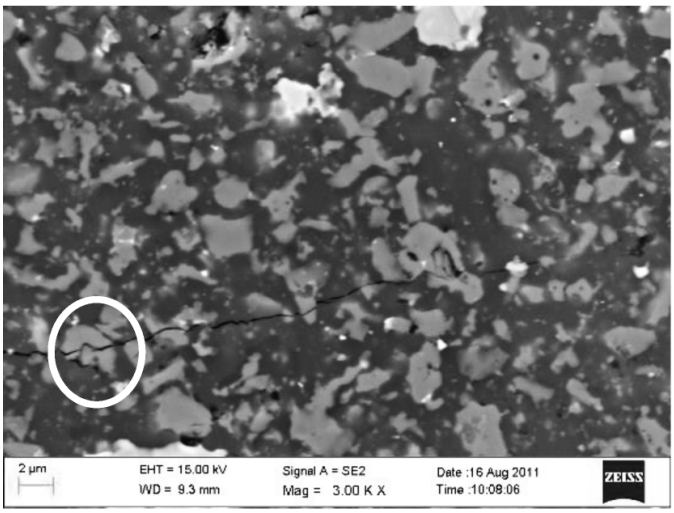

(e) 1700 ℃, polished surface, 3000×

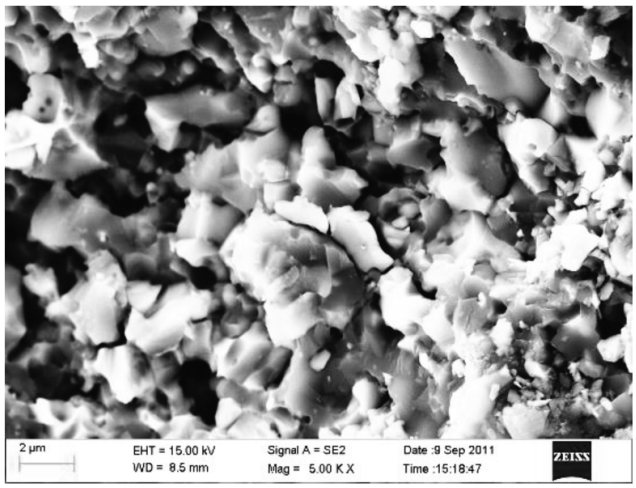

(f) 1700 ℃, fracture surface, 5000×

Fig. 3: Typical SEM micrographs of the materials (10 min, 32 MPa).

IV. Conclusions

The effects of sintering temperature on the phase composition, mechanical properties and microstructure of Al_2O_3-TiC-TiN ceramic tool materials were investigated.

The identified phases were analysed not only with regard to the crystal structures, but also the properties they might bring to the ceramic materials. It is inferred that hexagonal-Mo_3C_2 and tetragonal-$AlNi_3$ will adversely affect the mechanical properties overall. Orthorhombic-MoNi can improve the flexural strength and hardness. Cubic-$AlNi_3$ can enhance the strength and hardness of the material, but it reduces its fracture toughness.

The wetting effect of binding phase on the hard phase changed with the increment of the sintering temperature, the particle size and crack propagation path were also affected.

When the Al_2O_3-TiC-TiN ceramic materials were sintered with the holding time of 10 minutes and sintering pressure of 32 MPa, the highest flexural strength, the highest Vickers hardness, and the highest fracture toughness were measured when the sintering temperature was 1 650 °C, 1 700 °C, and 1 500 °C, respectively. The mechanical properties were overall optimal when the sintering temperature was 1 500 °C, at which the mechanical properties were 796.6 MPa, 20.5 GPa, 7.58 MPa·m$^{1/2}$ for flexural strength, Vickers hardness, and fracture toughness, respectively.

Acknowledgements

This work was supported by National Natural Science Foundation of China (Grant No. 51705286, 52075300); Natural Science Foundation of Shandong Province (Grant No. ZR2017BEE057,ZR2019MEE054); Major Program of Shandong Province Natural Science Foundation (Grant No. ZR2018ZA0401); Independent Training and Innovation Team Project of Jinan Science and Technology Bureau (Grant No. 2019GXRC009); Sichuan Province Science and Technology Support Program (Grant No. 2021YJ0056, 2021JDTD0025).

References

1 Su, Y.L.: Effect of the cutting speed on the cutting mechanism in machining CFRP, *J. Compos. Struct.*, **220**, 662 – 676, (2019).

2 Aslan, E.: Experimental investigation of cutting tool performance in high speed cutting of hardened X210 Cr12 cold-work tool steel (62 HRC), *Mater. Design.*, **26**, 21 – 27, (2005).

3 Godoy, V.A.A., Diniz, A.E.: Turning of interrupted and continuous hardened steel surfaces using ceramic and CBN cutting tools, *J. Mater. Process. Tech.*, **211**, 1014 – 1025, (2011).

4 Barry, J., Byrne, G.: Cutting tool wear in the machining of hardened steels: Part I: alumina/TiC cutting tool wear, *Wear*, **247**, 139 – 151, (2001).

5 Barry, J., Byrne, G.: Cutting tool wear in the machining of hardened steels: Part II: Cubic boron nitride cutting tool wear, *Wear*, **247**, 152 – 160, (2001).

6 Qiu, L.K., Li, X.K., Peng, Y., Ma, W.M., Qiu, G.M., Sun, Y.B.: Types, performance and application of Al_2O_3 system ceramic cutting tool, *J. Rare. Earth.*, **25**, 332 – 326, (2007).

7 Aslantas, K., Ucun, İ., Çicek, A.: Tool life and wear mechanism of coated and uncoated Al_2O_3/TiCN mixed ceramic tools in turning hardened alloy steel, *Wear*, **274 – 275**, 442 – 451, (2012).

8 Kumar, A.S., Durai, A.R., Sornakumar, T.: Machinability of hardened steel using alumina based ceramic cutting tools, *Int. J. Refract. Met. H.*, **21**, 109 – 117, (2003).

9 Cheng, Y., Hu, H.P., Sun, S.S., Yin, Z.B.: Experimental study on the cutting performance of microwave sintered Al_2O_3/TiC ceramic tool in the machining of hardened steel, *Int. J. Refract Met. H.*, **5**, 539 – 46, (2016).

10 Cheng, M.L., Liu, H.L. Zhao, B. Huang, C.Z., Yao, P., Wang, B.: Mechanical properties of two types of Al_2O_3/TiC ceramic cutting tool material at room and elevated temperatures, *Ceram. Int.*, **43**, 13869 – 13874, (2017).

11 Wang, D., Xue, C., Cao, Y., Zhao, J.: Microstructure design and preparation of Al_2O_3/TiC/TiN micro-nano-composite ceramic tool materials based on properties prediction with finite element method, *Ceram. Int.*, **44**, 5093 – 5101, (2018).

12 Sahoo, A.K., Sahoo, B.: Performance studies of multilayer hard surface coatings (TiN/TiCN/Al_2O_3/TiN) of indexable carbide inserts in hard machining: Part-I (An experimental approach), *Measurement*, **46**, 2854 – 2867, (2013).

13 Qiao, L.N., Zhao, Y.C. Wang, M.Z., Shi, C.J., Ye, Y.N., Zhang, J.X., Zou, Q., Yang, Q., Deng, H., Xing, Y.: Enhancing the sinter ability and fracture toughness of Al_2O_3-$TiN_{0.3}$ composites, *Ceram. Int.*, **42**, 3965 – 3971, (2016).

14 Shimada, S., Paseuth, A., Kiyono, H.: Coating and spark plasma sintering of nano-sized TiN on alumina particles of different size, shape and structure, *J. Ceram. Soc. Jpn.*, **117**, 47 – 51, (2009).

15 Kondo, M.Y., Pinheiro, C., Csouza, J.V., Ribeiro, M.V., Alves, M.C.S.: Optimizing cutting parameters for cutting power and roughness in VAT 32® turning with an experimental Al_2O_3-MgO ceramic tool using Taguchi's method, *Procedia CIRP.*, **77**, 610 – 613, (2018).

16 Azhar, A., Mohamad, H., Ratnam, M., Ahmad, Z.: The effects of MgO addition on microstructure, mechanical properties and wear performance of zirconia-toughened alumina cutting inserts, *J. Alloy. Compd.*, **497**, 316 – 320, (2010).

17 Fei, Y.H., Huang, C.Z., Liu, H.L., Zou, B.: The effect of MgO addition on the mechanical properties and phase composition of Al_2O_3 – TiC-TiN ceramic materials, *Adv. Mater. Res.*, **457 – 458**, 3 – 6, (2012).

18 Lu, X.X., Wang, W.H., Li, X.Y., Qiu, T.: Effect of MgO-Y_2O_3 on properties of Al_2O_3 materials prepared by hot-pressing sintering, (in Chinese), *J. Electronic components and materials*, **32**, 1 – 4, (2013).

19 Li, X.K., Qiu, G.M., Qiu, T., Zhao, H.T., Bai, H., Sun, X.D.: Al_2O_3/TiCN-0.2% Y_2O_3 composite prepared by HP and its cutting performance, *J. Rare. Earth.*, **25**, 37 – 41, (2007).

20 Ahamed, H., Senthilkumar, V.: Experimental investigation on newly developed ultrafine grained aluminium based nano composites with improved mechanical properties, *J. Mater. Design.*, **37**, 182 – 192, (2012).

21 Fei, Y.H., Huang, C.Z., Liu, H.L.: The phase composition and mechanical properties of Al_2O_3-TiN-TiC ceramic materials with different ni content, *J. Ceram. Sci. Tech.*, **10**, 55 – 62, (2019).

22 Fahrenholtz, W.G., Ellerby, D.T., Loehman, R.E.: Al_2O_3-ni composites with high strength and fracture toughness, *J. Am. Ceram. Soc.*, **83**, 1279 – 1280, (2000).

23 Fei, Y.H., Huang, C.Z., Liu, H.L., Zou, B.: The influence of ni addition on the microstructures and mechanical properties of Al_2O_3-TiN-TiC ceramic materials, *Nanomanuf. Metrol.*, **1**, 105 – 111, (2018).

24 Konopka, K., Maj, M., Kurzydłowski, K.J.: Studies of the effect of metal particles on the fracture toughness of ceramic matrix composites, *Mater. Charact.*, **51**, 335 – 340, (2003).

[25] Deng, J.X., Yang, X.F., Wang, J.H.: Wear mechanisms of Al_2O_3/TiC/Mo/Ni ceramic wire-drawing dies, *J. Mat. Sci. Eng. A.*, **424**, 347 – 354, (2006).

[26] Fei, Y.H., Huang, C.Z., Liu, H.L., Zou, B.: Mechanical properties of Al_2O_3-TiC-TiN ceramic tool materials, *Ceram. Int.*, 40, 10205 – 10209, (2014).

[27] Fei, Y.H., Huang, C.Z., Liu, H.L., Zou, B.: Study on the cutting performance of Al_2O_3-TiC-TiN ceramic tool material, *Key Eng. Mater.*, **40**, 10205 – 10209, (2016).

[28] Shi, D.M., Wen, B., Melnik, R., Yao, S., Li, T.J.: First-principles studies of al-ni intermetallic compounds, *J. Solid. State. Chem.*, **182**, 2664 – 2669, (2009).

[29] Rödel, J., Prielipp, H., Claussen, N., Sternitzke, M., Alexander, K.B., Becher, P.F., Schneibel, J.H.: Ni_3Al/Al_2O_3 composites with interpenetrating networks, *Scripta Metall. Mater.*, **33**, 843 – 848, (1995).

[30] Adabi, M., Amadeh, A.: Formation mechanisms of Ni-Al intermetallics during heat treatment of Ni coating on 6061 Al substrate, *T. Nonferr. Metal. Soc.*, **25**, 3959 – 3966, (2015).

[31] Scudino, S., Sperling, S., Sakaliyska, M., Thomas, C., Feuerbacher, M., Kim, K.B., Ehrenberg, H., Eckert, J.: Phase transformations in mechanically milled and annealed single-phase β-Al_3Mg_2, *Acta. Mater.*, **56**, 1136 – 1143, (2008).

[32] Straumal, B.B., Baretzky, B., Kogtenkova, O.A., Straumal, A., Sidorenko, A.: Wetting of grain boundaries in al by the solid Al_3Mg_2 phase, *J. Mater. Sci.*, **45**, 2057 – 2061, (2010).

[33] Hugosson, H.W., Eriksson, O., Nordström, L.: Theory of phase stabilities and bonding mechanisms in stoichiometric and substoichiometric molybdenum carbide, *J. Appl. Phys.*, **86**, 3758 – 3767, (1999).